Western North American Naturalist 60(2), © 2000, pp. 111–120

A GIS MODEL TO PREDICT THE LOCATION OF FOSSIL PACKRAT (*NEOTOMA*) MIDDENS IN CENTRAL NEVADA

Scott A. Mensing[1], Robert G. Elston, Jr.[1], Gary L. Raines[2], Robin J. Tausch[3], and Cheryl L. Nowak[3]

ABSTRACT.—Fossil packrat (*Neotoma*) middens provide an important source of paleoecologic data in the arid West. This study describes and tests a predictive GIS model that uses the weights-of-evidence method for determining areas with a high probability of containing fossil middens in central Nevada. Model variables included geology, elevation, and aspect. Geology was found to be the most important variable tested. We produced a map of 4 probability classes validated by field-checking 21 randomly selected 1-km^2 sites throughout the study area. Our high-probability category reduced the search area to only 3.5% of the total study area. Fossil middens were found on 8 of 21 sites (38%). Geologic types that contained middens were granite, limestone, and volcanic tuff. A 2nd run of the model with the new midden localities added to the training set helped narrow the total search area even further. This analysis demonstrates that the weights-of-evidence method provides an effective tool both for guiding research design and for helping locate midden sites within specific localities. With only a limited training dataset and a simple set of mapped criteria, a model can be constructed that is both predictive and testable. We intend to continue development of the model to improve our ability to predict the location of Pleistocene-age middens and to locate middens on low-probability sites. This method, designed for mineral exploration, has wide potential application within the natural sciences.

Key words: GIS predictive model, weights-of-evidence, fossil packrat middens, Nevada, Neotoma.

Plant and animal macrofossils preserved in fossilized packrat (*Neotoma*) middens are an important source of evidence for reconstructing paleoclimate and vegetation change in the arid West (Betancourt et al. 1990). Middens contain plant fragments, fecal pellets, bone fragments, and other debris collected within approximately a 1-ha area of a *Neotoma* den (Finley 1990, Spaulding et al. 1990). *Neotoma* spp. repeatedly urinate on their collections and, over time, the mass hardens into a material called amberat, which protects the midden contents from decay. A den may be abandoned and reinhabited many years later, leading to the accumulation of multiple strata in the midden. Middens can be as large as 7 m high and 10 m wide, but middens of 1–2 m are more common. Although *Neotoma* inhabit a broad range of habitats and are widely distributed (Vaughan 1990), fossil middens are found only in sites sheltered from rain and runoff, such as caves or under overhanging rocks, because amberat dissolves in water.

Characteristics that define fossil midden locations in the Great Basin are cave-forming substrate, mid-elevations, and southwest to easterly exposure (Webb and Betancourt 1990). On some rocky sites Holocene middens are very common. However, the Great Basin is geologically complex, and sites where fossil middens are abundant are often widely separated. One of our research goals was to reconstruct plant species migration patterns over distance and elevation across the central Great Basin. This effort requires a high-resolution spatial network of fossil middens. Much of central Nevada has limited road access, and systematically searching all potential midden localities is logistically prohibitive. A predictive model that maps the probability of finding fossil middens would both focus search efforts, increasing the efficiency of valuable field time, and identify new areas that may not have been expected to have middens.

Geographic information systems (GIS) models have been used to predict locations of rare orchid habitat (Sperduto and Congalton 1996), black bear habitat (van Manen and Pelton 1997), squirrel distribution (Rushton et al. 1997), breeding bird distributions (Tucker et al. 1997),

[1]Department of Geography, University of Nevada, Reno, NV 89557.
[2]United States Geological Survey and Adjunct Faculty, Department of Geosciences, University of Nevada, Reno, NV 89557.
[3]USDA Forest Service, Rocky Mountain Research Station, 920 Valley Road, Reno, NV 89512.

and rare mineral deposits, particularly gold (Bonham-Carter et al. 1988, Agterberg et al. 1990, Xu et al. 1992). In this paper we present a GIS model to predict the location of fossil *Neotoma* midden sites in central Nevada. The goal of this study was to test the effectiveness of this approach for identifying specific search locations within a very large study area. Once developed, and with additional data, such a model could then be refined to improve our ability to find Pleistocene-age middens or to identify potential sites in localities where fossil middens are less common.

METHODS

Weights-of-Evidence Method

Weights-of-evidence is a quantitative method originally designed as a medical data-driven system for combining information about symptoms to predict disease (Xu et al. 1992, Bonham-Carter 1994). The method was adapted for mineral exploration using geologic and geochemical datasets to predict the location of specific ore deposits (Bonham-Carter et al. 1988). Recently, a software package for calculating weights-of-evidence was developed as an extension to run with the ArcView™ Spatial Analyst GIS program (ESRI, Redlands, CA). A beta version of the weights-of-evidence ArcView™ extension (Kemp et al. 1999) was used in this research.

The weights-of-evidence program uses a set of training points (in this case, known fossil midden locations), a spatially defined study area, and a set of thematic maps (evidential themes), which represent variables that are considered predictive of the training point data. Evidential themes are assumed to be conditionally independent with respect to training points. Training points are compared against each evidential theme to calculate the measure of spatial association between the points and each class or attribute in the theme. A weight is calculated for each class in a theme, with a positive weight (W^+) if the class is present and a negative weight (W^-) if the class is absent. The difference between weights is the contrast (Bonham-Carter 1994), which measures the strength of the correlation between the training set and classes in the theme. Positive contrast values suggest that more training points occur in that class than would be expected by chance, and negative contrast values suggest fewer training points than would exist by chance alone. Equations for the derivation of contrast are described in detail in Bonham-Carter et al. (1988), Bonham-Carter (1994), and Kemp et al. (1999). Positive contrast values of 0–0.5 are usually considered mildly predictive, 0.5–1.0 moderately predictive, 1.0–2.0 strongly predictive, and >2.0 extremely predictive (Bonham-Carter 1994). Contrast values are used to reclassify each evidential theme into a binary map with only 2 classes, 'inside' or predictive and 'outside' or not predictive. The user's decisions on how high or low to set the predictive values in each evidential binary map influence the model outcome.

Before running the model, the program calculates prior probability by dividing number of training points, where each point represents a user-defined unit area, by total study area, assuming a random distribution of sites. This probability will invariably be less than the spatial density of all existing middens because the training set represents a small sample of existing middens in a large study area. However, it provides an initial probability to start the modeling. Evidential binary maps are then combined to give the posterior probability to each cell for each unique binary combination. For example, if 3 themes were combined, any cell containing the predictive variable, 'inside', in all 3 themes would have the highest posterior probability. Overlaying cells with 'inside' in 2 themes and 'outside' in 1 theme would meet only 2 predictive criteria and have a lower probability. Posterior probabilities higher than the prior probability suggest a nonrandom distribution and indicate that locations of training points are controlled by specific environmental variables.

To create a map that represents true probability, each evidential theme must be conditionally independent with respect to training points; however, this assumption is probably always violated to some extent (Bonham-Carter 1994). Weights-of-evidence software incorporates a test for conditional independence, which calculates the ratio between actual number and predicted number of training points. A value of 1 means the evidential themes are conditionally independent with respect to training points; a value of 0 means there is absolute dependence. Values >0.85 are generally considered acceptable for demonstrating

conditional independence (Agterberg 1994 personal communication).

Fossil Midden Training Dataset and Study Area

The training point dataset included 346 fossil midden samples from central Nevada. Fourteen samples had no location data and were discarded. Duplicate samples and middens from the same location were also discarded, reducing the dataset to 85 locations. These locations were then entered into the ArcView™ GIS program. Points were plotted on the 1:500,000 scale geology of Nevada (Stewart and Carlson 1978) and checked for accuracy. In several cases the location was on the wrong geologic type as recorded from field notes by the midden collector. This typically occurred in areas of complex geology where spatial resolution of the geologic map was insufficient to capture variability on the ground, making the midden location appear on the wrong geologic type. In these cases the midden location was moved to the correct geology. In general, points were not shifted more than 200 m, which is less than the spatial resolution of the 1:500,000-scale geology theme. Original aspect and elevation were unchanged.

A 1-km^2 lattice, representing the minimum spatial resolution of the weights-of-evidence model, was then laid over the geology. Where more than 1 training point occurred on the same geology within a 1-km^2 cell, duplicate points were discarded. The weights-of-evidence method calculates the posterior probability of a point occurring in a unit cell, 1 km^2 in this case. Consequently, the method cannot consider multiple points per cell, which is a limitation of the method. The final training point dataset had 60 midden locations. Only 58 points were used in model 1 because 2 middens fell outside the study area. If these 58 training points somehow are a biased sample, for example, if a particular geologic unit or elevation were never sampled, then the resulting model will be influenced by this bias. The authors are unaware of any bias in this sample of midden locations.

The study area was restricted to central Nevada counties where our training points were concentrated (Fig. 1). All major geologic formations in the state and many of the largest mountain ranges are found in this region. Elevation as calculated by the digital elevation model ranged from 1000 m in Dixie Valley to 3949 m at Wheeler Peak in Great Basin National Park.

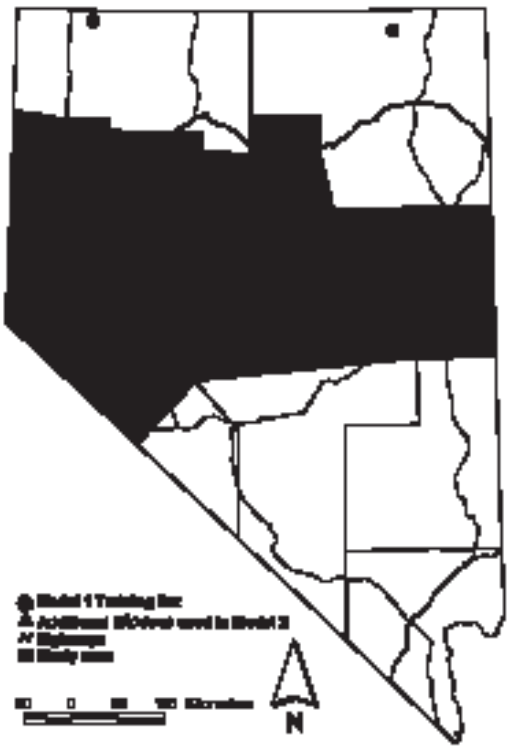

Fig. 1. Map of the model study area with training point locations. Open circles represent the original training set used to create model 1. Open triangles represent middens found during field validation of model 1 and added to the original training set to create model 2.

Creation of Evidential Themes

Four evidential themes were considered for this model: geology, elevation, slope, and aspect. These themes provide information on the 3 major characteristics of midden locations: substrate, elevation, and exposure.

The geology evidential theme was created from the 1:500,000 U.S. Geological Survey geologic map of Nevada (Stewart and Carlson 1978). Large-scale geologic maps (>1:100,000) would have included smaller features and isolated rock outcrops; however, coverage of the study area was unavailable at these scales. Geology at a 1:250,000 scale was available, but it was constructed from 13 county maps with different definitions of geologic formations. Consequently, geologic map units did not

match across county lines and were inconsistent across the state. Only the 1:500,000 scale provided a consistent geologic base map across the entire study area. The original vector coverage was rasterized by use of 276 × 276-m pixels. This cell size was selected to adequately represent the information content of the geologic map. Weights-of-evidence does not require that evidential themes be degraded to a consistent cell size. The user-defined unit cell, 1 km^2, defines that each training point will be counted as 1 km^2 and evidential themes will be measured in units of 1 km^2.

We were concerned that the 1:500,000-scale map would lack resolution necessary to identify small outcrops of suitable geology that fell below the minimum mapping resolution threshold. To test the loss of resolution associated with moving to a small-scale map, we compared minimum mapping resolution and changes in lithologic boundaries between 3 map scales, the Austin 1:62,500 quadrangle (McKee 1978), Lander County 1:250,000 map (Stewart and McKee 1977), and USGS 1:500,000 Nevada map (Stewart and Carlson 1978). The test area contained 6 midden sites, 4 of which were mapped on granitic rock and 2 on limestone. Granitic formations remained consistent through all 3 map scales, including general polygon size and lithologic boundary. A section of Quaternary alluvium at the base of the granitic rock was mapped as a 200-m-wide strip at 1:62,500 scale, but shrank to a 100-m-wide strip at 1:250,000 scale and disappeared altogether at 1:500,000 scale. Loss of this detail did not influence the geologic type associated with midden sites. Limestone was mapped as 4 distinct units with 2 different named formations on the 1:62,500 map. The 1:250,000-scale map had 2 formations and only 2 rock units. At the 1:500,000 scale the limestone had been reduced to 1 named formation and 1 mapped unit; however, middens were still located on the correct lithology. Although our analysis was necessarily limited due to a lack of 1:62,500 geologic maps, it demonstrated that the 1:500,000 map was consistent with larger-scale maps.

Aspect, slope, and elevation evidential themes were constructed from a U.S. Geological Survey digital elevation model (DEM) of Nevada with an initial cell size of 92 m. Cell size was resampled to 276 m to be consistent with the geology theme. The elevation evidential theme was created by classifying the DEM into 30 elevation classes of 98.3 m each. Aspect and slope evidential themes were derived from the DEM by use of the ArcView™ Spatial Analyst algorithms. Aspect was classified into 16 classes with 22.5° in each class. Slope and geology were found to be conditionally dependent with respect to middens, and slope was eliminated from the model.

Weighting of Evidential Themes

Contrast values were calculated for geology, elevation, and aspect evidential themes. In selecting optimal weights for creating binary evidential maps, we took a conservative approach and restricted the model to classes with highest contrast values.

Training points occurred on 23 of 85 geologic types in the study area (model 1, Table 1). Four geologic types had contrast values <0.5, five had values of 0.5–1.0, seven had values of 1.0–2.0, and 7 had values >2.0. The 15 geologic types with contrast ≥ 0.966 (strongly predictive) were classified as 'inside' for model 1, and the remaining 70 were classified as 'outside'. Of 58 training sites, 42 (72%) fell within these 15 geologic types. This criterion was used to provide a prediction that was tightly focused on the most favorable geologic types.

Model 1 contrast values for aspect and elevation are graphed in Figure 2. For aspect classes 4–10, representing compass bearings from east-northeast to south-southwest (67.5°–247.5°), contrast was generally positive with moderate to strongly predictive values. The negative value for class 6 (east-southeast aspect) was disregarded as a minor deviation in an otherwise continuous interval. This aspect may represent minor sampling bias in the training set. Aspect classes 4–10 were classified as 'inside' and all other aspects as 'outside'. Of 58 training sites, 41 points (71%) fell within this range of aspects.

Elevation had a bimodal distribution, with classes 6–7 and 11–14 (1492–1688 m and 1983–2376 m) having positive contrast values and most other elevation classes having negative or only weakly positive contrast values (Fig. 2). Contrast values in these 2 class ranges were moderate to strongly predictive. Thirty-nine (67%) training points were associated with these elevation classes. The gap between 1688 and 1983 m may be an artifact of a limited set

TABLE 1. Variation of weights-of-evidence for geologic type ranked by contrast value. Note that the rank for contrast value changes under model 2. The points column is the number of cells containing a training point. Geologic descriptions are Tmi, intrusive mafic; Jd, JTRsv, Osv, Ts3, sedimentary/tuff; Tgr, Kgr, MZgr, granitic; Jgb, Tb, Tba, basalt; Tr2, Tr1, intrusive/rhyolitic; Tt3, Tt2, TRk, volcanic tuff; Dc, Oc, Os, PPc, JTRs, MDs, sedimentary/limestone; and Ta3, andesite.

		Model 1		Model 2	
Geology	Area (km^2)	Points	Contrast	Points	Contrast
Tmi	44	3	5.077	3	4.836
Jd	142	1	2.703	1	2.469
Tgr	229	1	2.223	3	3.125
Jgb	241	1	2.170	1	1.936
Tr2	252	1	2.123	1	1.893
Kgr	2015	7	2.089	11	2.347
Tt3	266	1	2.071	1	1.837
Tb	2111	5	1.665	5	1.416
Dc	1727	4	1.628	6	1.818
TRk	424	1	1.604	1	1.370
JTRsv	1185	2	1.278	3	1.461
Oc	1190	2	1.274	6	2.197
MZgr	2099	3	1.122	4	1.184
Tba	4676	6	1.049	6	0.795
Ta3	3298	4	0.966	5	0.959
Os	991	1	0.746	1	0.513
PPc	994	1	0.744	1	0.510
JTRs	2020	2	0.737	2	0.499
Osv	1100	1	0.641	1	0.407
Tr1	1319	1	0.458	1	0.224
MDs	1415	1	0.387	1	0.153
Tt2	10651	7	0.345	7	0.087
Ts3	4004	2	0.035	2	–0.201

of training sites. However, another possibility relates to topography. The base elevation for mountain ranges in central and eastern Nevada is higher than in the western part of the state. The 1688–1983 m elevation range approximately coincides with the elevation of basin floors and alluvial fans in central and eastern Nevada. These geomorphic features rarely preserve fossil middens due to repeated periods of erosion and deposition. For the purpose of constructing the model, we followed the data and classified elevations 6–7 and 11–14 as 'inside' and all others as 'outside'.

Validation

To validate the model, we randomly selected a set of 1-km^2 sites to field-search. We placed a 1-km^2 lattice within an 8-km buffer of all major roads in the study area. In testing the model, we chose to follow a conservative, practical approach. If a randomly chosen 1-km^2 site inside the 8-km buffer had at least 3 high-probability cells (approximately 25% of the plot), it was considered a high-probability site and included for field-checking. We selected 75 sites for potential field-checking. Selected sites averaged 6 high-probability cells (approximately 50% of the plot). The intent of the model was to guide a user to the best potential sites for collecting fossil middens. We felt that if at least 25% of any given 1-km^2 area was predicted to have middens, that was sufficient information to locate a site that should contain fossil middens.

We selected both a moderate- and low-probability site within a 25-km^2 matrix near each high-probability site to test the accuracy of our predictive criteria. The 25-km^2 matrix was subjectively placed so that secondary sites were never farther from a main road than the primary site. Within this matrix, however, secondary sites were randomly selected. If no moderate- or low-probability sites were available within the matrix, then the nearest available site was chosen. We chose this approach for efficiency. The study area covered 120,000 km^2, and although secondary sites may not be truly independent, we wanted to visit the maximum number of sites within the limited time available for fieldwork.

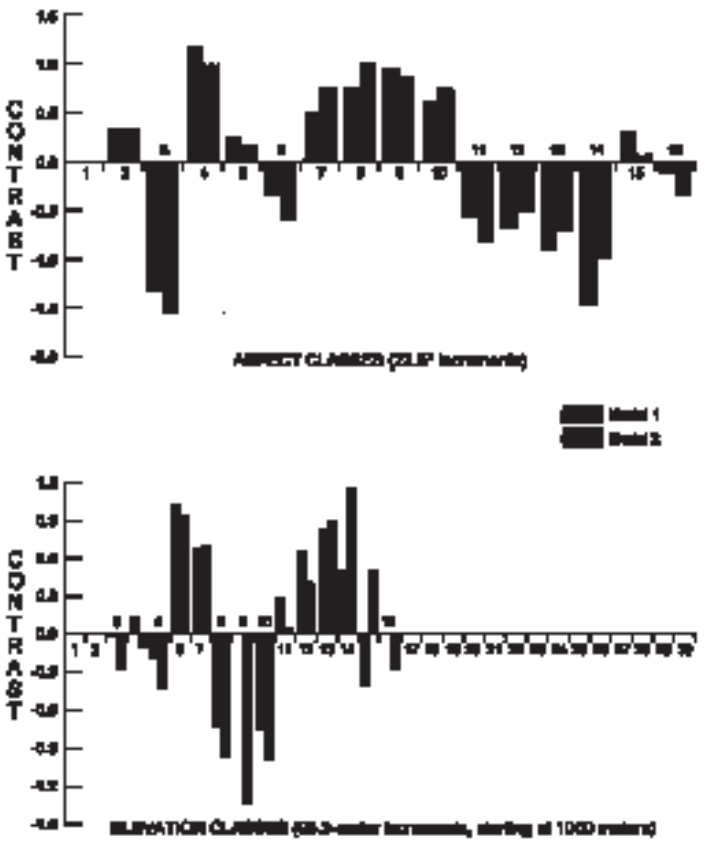

Fig. 2. Contrast values for aspect and elevation evidential themes for model 1 and model 2. Abscissas represent the entire range found in the study area. Aspect classes represent 22.5° increments (1 = 0°–22.5°, 2 = 22.5°–45°, etc.). Elevation classes represent 98.3-m increments.

At each validation site we walked the entire 1-km^2 plot looking for collectible fossil middens, defined as having a brown to black weathering rind and a volume of no less than 1–2 L. In a few cases poor road access and vertical terrain prevented searching on foot. Here we used high-powered sighting scopes to search the site. Our experience has shown that caves with middens can be positively identified with this method, although we verified such sightings on foot whenever possible. In only 1 case did we sight middens through the scope that we could not actually get close to for positive identification, and this was on a moderate-probability site. New midden locations found during the validation process were added to the training set for the 2nd model run.

RESULTS

Two models predicting distribution of middens were created from reclassified evidential themes. Model 1 had an acceptable conditional independence ratio of 0.87. Prior probability of a random cell containing a fossil packrat midden was 0.0005. Posterior probability for each combination of class values is given in the unique conditions table (Table 2). Geology was clearly the most important variable in determining probability of fossil midden locations (Table 3). For purposes of this study, we considered ranking of probabilities as sufficient.

Under the model all cells that were strongly predictive for all 3 themes, geology, aspect, and elevation, had a probability of 0.0067. Nineteen training points (33%) were in this category.

TABLE 2. Unique conditions table for the 3 evidential themes, geology, elevation, and aspect, used in model 1 and model 2 where 2 = desired condition present and 1 = desired condition absent. The points column is the number of training points with that unique condition. Value simply ranks each unique condition by probability.

Value	Geology	Elevation	Aspect	Points	Area (km^2)	Probability
MODEL 1						
1	2	2	2	19	4,285	0.0067
2	2	2	1	7	4,710	0.002
3	2	1	2	10	5,044	0.002
4	2	1	1	6	5,845	0.0005
5	1	2	2	11	14,727	0.0005
6	1	2	1	2	19,336	0.00015
7	1	1	2	1	25,397	0.00014
8	1	1	1	2	40,765	0.00004
MODEL 2						
1	2	2	2	23	2,908	0.0123
2	2	2	1	8	3,113	0.0035
3	2	1	2	10	2,787	0.0031
4	2	1	1	5	3,105	0.0009
5	1	2	2	15	17,551	0.0008
6	1	2	1	6	22,553	0.0002
7	1	1	2	4	26,208	0.0002
8	1	1	1	2	41,886	0.00006

These cells represented the highest probability of containing a fossil midden according to the model and were classified as high (Fig. 3). Total area of high-probability cells was 4285 km^2, equal to 3.5% of the study area.

Cells that were strongly predictive for geology plus either elevation or aspect had a probability of 0.002. Seventeen training points (29%) were in this category. The probability of a midden's being on these sites was higher than the prior probability that assumed random distribution, and these cells were classified as moderate.

If a cell was only strongly predictive for geology, or elevation and aspect, the probability of its containing a midden was no better than random (0.0005), and these sites were classified as low. Another 17 training points (29%) were in this category. The remaining area had a posterior probability (0.00014) below the prior probability, and these sites were classified very low. Five training points (9%) were in this category. The map of probability classes (Fig. 3) was used to select sites to validate the model.

We field-checked 21 of 75 sites randomly selected from across the entire study area. Limited field time (6 d) and difficult access over a large area prevented us from visiting more sites. Sixteen sites were on limestone/sedimentary (Oc, Dc), granite (Kgr, Tgr, MZgr), or andesite/volcanic tuff (Ta3), and 5 sites were on basalt (Tb). The 6 other geologic types used in the model (Tmi, Jd, Jgb, Tr2, Tt3, and TRk) are each limited in extent (total area for these rock types ranged between 43 and 425 km^2). None of the randomly chosen sites fell on these geologic types.

Fossil middens were found on 8 of 21 sites (38%). This percentage is significantly higher than the probability predicted by the model ($\chi^2 = 422.48$, 1 df, $P < 0.001$). Of these 8 sites, all had middens on the high-probability plots, 5 had middens on moderate-probability plots, and 2 on low-probability plots for a total of 15 new midden locations. Four sites (8 middens) were on granitic rock, 3 (6 middens) on limestone/sedimentary, and 1 (1 midden) on a volcanic welded tuff. None of the basalt sites held middens.

We added the 15 new midden sites discovered in validating model 1 to the training set and reran the model to test whether contrast

TABLE 3. Weights and contrast values for each evidential theme used in model 1. Each theme is reclassified into a binary map prior to running the model using the classes 'inside' or predictive (W^+) and 'outside' or not predictive (W^-). A strongly predictive theme produces a higher contrast value.

Theme	W^-	W^+	Contrast
Geology	–0.8905	1.8519	2.7424
Elevation	–0.7609	0.6192	1.3801
Aspect	–0.7149	0.5494	1.2643

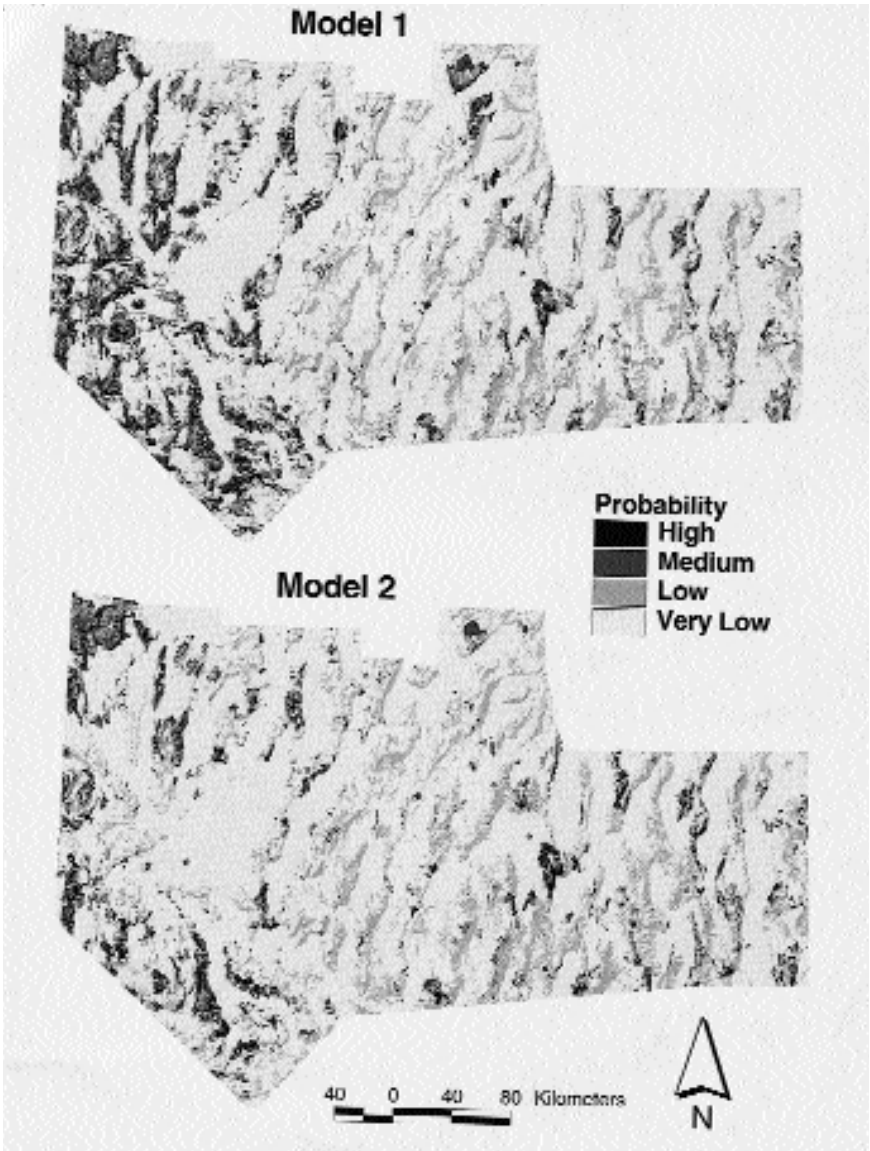

Fig. 3. Map of probability classes for model 1 and model 2 (levels are defined in the text).

values strengthened and posterior probability improved. As expected, contrast values changed for geologic types with additional training points (model 2, Table 1). The order of rank also changed; however, the 15 geologic types used in the 1st model still had highest overall contrast values. For model 2, contrast values >1.0 were classified as 'inside' for geology, which removed Ta3 from the predictive set. The large area (3298 km^2) coupled with low number of points (5 training points) makes this geologic type only moderately predictive. With more training points this geologic type may prove to be a reliable predictor.

Contrast values for aspect and elevation are graphed in Figure 2. For aspect, classes 4–10, representing compass bearings from east-northeast to south-southwest (67.5°–247.5°), continued to have highest contrast and were classified as 'inside'. The addition of sites at higher elevations shifted significant elevation classes so that classes 6–7 and 11–15 (1492–1688 m and 1983–2474 m) were classified as 'inside'.

Prior probability for model 2 improved to 0.0006. The test for conditional independence returned a value of 0.86, an acceptable level of conditional independence. Posterior probability for each possible combination of class values is given in the unique conditions table (Table 2). Posterior probability values were mapped as 4 generalized classes, >0.004 (high), >0.001 and ≤0.004 (moderate), >0.0003 and ≤0.001 (low), and ≤0.0003 (very low; Fig. 3). Posterior probability for cells with optimal geology, aspect, and elevation was 0.012. Probability was higher than in model 1 because total area within the highest probability was reduced to 2908 km^2 (2.4% of the total study area) and number of training points increased from 19 to 23. Eighteen training points (25%) were on cells with a probability of 0.0031–0.0039 that we ranked as moderate because the value was greater than prior probability but lower than highest probability. Twenty sites (27%) were located on cells with a probability roughly equivalent to prior probability and were ranked low, and 12 sites (16%) were below prior probability

DISCUSSION AND CONCLUSIONS

Our purpose was to construct a GIS model from a small training set that would rank suitable sites for finding fossil *Neotoma* middens across a large portion of Nevada. The model performed well in both limiting the area to search and guiding us to collectible fossil middens. The high-probability category in model 1 reduced the search area to 3.5% of the total study area. Field validation of the model found fossil middens on 38% of the sites. This percentage was significantly higher than the probability predicted by the model and suggests that middens are particularly common on high-probability sites. A 2nd model with additional data changed probability values. Additional training data would likely result in a refinement of the ranking of key geologic types, improving the model as a field research tool.

The model performed well ranking the probability of potential midden occurrence within a site. Eight field-checked sites had middens on high-probability sites. Only 5 of these also had middens on moderate-probability sites, and 2 had middens on low-probability sites. In no cases did we find middens at low- or medium-probability sites but not at high-probability sites. This suggests that when the model predicts an area is likely to have middens, they may also be found in proximity to highest probability sites, although the greatest likelihood of finding a midden is on high-probability sites.

We have demonstrated that the model can accurately predict the most common sites for fossil middens. Our goal now is to refine the model and improve our ability to predict very old middens and middens on low-probability sites. Pleistocene-age middens tend to be in more specialized locations, and as more data become available, the model could be refined to focus on these sites. Approximately 40% of training points ended up on sites with low or very low probability of having middens. We need to examine additional evidential themes that may help predict middens on these types of sites. For example, our field-testing included 5 sites on basalt, none of which contained middens. Although basalt had a relatively high contrast value in the initial model, fossil middens are usually found at the edge of flows where cliff faces form. Much of the area dominated by flood basalts in Nevada may have little chance of containing a midden; however, if we can use GIS to identify cliff faces within basalt, we may increase the probability of finding middens associated with this geology. Basalt and andesite cover large portions of western Nevada and have potential for containing fossil middens. These geologic types and others warrant further research to improve our search criteria.

The weights-of-evidence method used in this analysis demonstrates that with a limited set of known sites, and a simple set of search criteria in the form of digital maps, a well-defined model can be constructed that is both predictive and testable. A larger training dataset can potentially produce a model with very high predictive value. Although the software was designed for mineral exploration, it has been successfully applied in a biological context. The method has wide potential application for problems requiring identification and understanding of habitat for specialized taxa, or for a variety of exploration questions, including finding populations of rare and endangered species or identifying potential archaeological sites. Continued development of high-resolution digital datasets will enhance our

ability to improve field exploration through the use of geographic information systems.

ACKNOWLEDGMENTS

We thank Al Brunner for mapping existing midden locations and Craig Biggart and Stephanie Jensen for assisting with locating middens in the field. Bob Nowak provided *Neotoma* midden site data. We thank Frank van Manen and an anonymous reviewer for their comments. Peter Wigand provided suggestions on an earlier version of the manuscript. Funding was provided by United States Department of Agriculture Cooperative State Research, Education and Extension Service, Grant 95-37101-2027.

LITERATURE CITED

AGTERBERG, F.P., G.F. BONHAM-CARTER, AND D.F. WRIGHT. 1990. Statistical pattern integration for mineral exploration. Pages 1–21 *in* G. Gaal and D.F. Merriam, editors, Computer applications in resource estimation: prediction and assessment for metals and petroleum. Pergamon, Oxford, United Kingdom.

BETANCOURT, J.L., T.R. VAN DEVENDER, AND P.S. MARTIN. 1990. Packrat middens; the last 40,000 years of biotic change. University of Arizona Press, Tucson. 467 pp.

BONHAM-CARTER, G.F. 1994. Geographic Information Systems for geoscientists: modeling with GIS. Pergamon, Oxford, United Kingdom. 398 pp.

BONHAM-CARTER, G.F., F.P. AGTERBERG, AND D.F. WRIGHT. 1988. Integration of geological datasets for exploration in Nova Scotia. Photogrammetric Engineering and Remote Sensing 54:695–700.

FINLEY, R.B. JR. 1990. Woodrat ecology and behavior and the interpretation of paleomiddens. Pages 28–42 *in* J.L. Betancourt, T.R. Van Devender, and P.S. Martin, editors, Packrat middens; the last 40,000 years of biotic change. University of Arizona Press, Tucson.

KEMP, L., G.F. BONHAM-CARTER, AND G.L. RAINES, 1999. Arc-WofE: Arcview extension for weights of evidence mapping: http://gis.nrcan.gc.ca/software/arcview/wofe

MCKEE, E.H. 1978. Geologic map of the Austin Quadrangle, Lander County, Nevada (map at scale 1:62,500). Department of the Interior, United States Geological Survey, Reston, VA.

RUSHTON, S.P., P.P.W. LURZ, R. FULLER, AND P.J. GARSON. 1997. Modelling the distribution of the red and grey squirrel at the landscape scale: a combined GIS and population dynamics approach. Journal of Applied Ecology 34:1137–1154.

SPAULDING, W.G., J.L. BETANCOURT, L.K. CROFT, AND K.L. COLE. 1990. Packrat middens: their composition and methods of analysis. Pages 59–84 *in* J.L. Betancourt, T.R. Van Devender, and P.S. Martin, editors, Packrat middens; the last 40,000 years of biotic change. University of Arizona Press, Tucson.

SPERDUTO, M.B., AND R.G. CONGALTON. 1996. Predicting rare orchid (small whorled pogonia) habitat using GIS. Photogrammetric Engineering and Remote Sensing 62:1269–1279.

STEWART, J.H., AND J.E. CARLSON. 1978. Geologic map of Nevada (map at scale 1:500,000). Department of the Interior, United States Geological Survey (in cooperation with the Nevada Bureau of Mines and Geology), Reston, VA. *In:* G.L Raines, D.L Sawatsky, and K.A. Conners, 1996, Great Basin geoscience data base: United States Geological Survey Digital Data Series 41. Department of the Interior, United States Geological Survey. Reston, VA.

STEWART, J.H., AND E.H. MCKEE. 1977. Geology and mineral deposits of Lander County, Nevada; Nevada Bureau of Mines and Geology Bulletin 88, plate 1 (map at scale 1:250,000). Nevada Bureau of Mines and Geology, Reno. *In:* R.H. Hess and G. Johnson, 1997, NBMG Open-File report 97-1: county digital geological maps. Nevada Bureau of Mines and Geology, Reno.

TUCKER, K., S.P. RUSHTON, R.A. SANDERSON, E.B. MARTIN, AND J. BLAIKLOCK. 1997. Modelling bird distributions—a combined GIS and Bayesian rule-based approach. Landscape Ecology 12:77–93.

VAN MANEN, F.T., AND M.R. PELTON. 1997. A GIS model to predict black bear habitat use. Journal of Forestry 95:6–12.

VAUGHAN, T.A. 1990. Ecology of living packrats. Pages 14–27 *in* J.L. Betancourt, T.R. Van Devender, and P.S. Martin, editors, Packrat middens; the last 40,000 years of biotic change. University of Arizona Press, Tucson.

WEBB, R.H., AND J.L. BETANCOURT. 1990. The spatial and temporal distribution of radiocarbon ages from packrat middens. Pages 85–103 *in* J.L. Betancourt, T.R. Van Devender, and P.S. Martin, editors, Packrat middens; the last 40,000 years of biotic change. University of Arizona Press, Tucson, Arizona.

XU, S., Z. CUI, X. YANG, AND G. WANG. 1992. A preliminary application of weights of evidence in gold exploration in Xion-er Mountain Region, He-Nan Province. Mathematical Geology 24:663–674.

Received 12 January 1999
Accepted 23 August 1999